BNL-76920-2006-JA

STUDIES OF DIESEK ENGINE PARTICLE EMISSIONS DURING TRANSIENT OPERATIONS USING AN ENGINE EXHAUST PARTICLE SIZER

J. Wang, J. Storey, N. Domingo, S. Huff, J. Thomas, and B. West

Accepted for publication in
Aerosol Science and Technology
(in press)

May 2006

Environmental Sciences Department/Atmospheric Sciences Division

Brookhaven National Laboratory
P.O. Box 5000
Upton, NY 11973-5000
www.bnl.gov

Studies of diesel engine particle emissions during transient operations using an Engine Exhaust Particle Sizer

Jian Wang[1*], John Storey[2], Norberto Domingo[2],
Shean Huff[2], John Thomas[2], and Brian West[2]

[1]Brookhaven National Laboratory, Upton, NY 11973
[2]Oak Ridge National Laboratory, Oak Ridge, TN 37831

Abstract

Diesel engine particle emissions during transient operations, including emissions during FTP transient cycles and during active regenerations of a NOx adsorber, were studied using a fast Engine Emission Particle Sizer (EEPS). For both fuels tested, a No. 2 certification diesel and a low sulfur diesel (BP-15), high particle concentrations and emission rates were mainly associated with heavy engine acceleration, high speed, and high torque during transient cycles. Averaged over the FTP transient cycle, the particle number concentration during tests with the certification fuel was 1.2e8/cm^3, about four times the particle number concentration observed during tests using the BP-15 fuel. The effect of each engine parameter on particle emissions was studied. During tests using BP-15, the particle number emission rate was mainly controlled by the engine speed and torque, whereas for Certification fuel, the engine acceleration also had a strong effect on number emission rates. The effects of active regenerations of a diesel NOx adsorber on particle emissions were also characterized for two catalyst regeneration strategies: Delayed Extended Main (DEM) and Post 80 injection (Post80). Particle volume concentrations observed during DEM regenerations were much higher than those during Post80 regenerations, and the minimum air to fuel ratio achieved during the regenerations had little effect on particle emission for both strategies. This study provides valuable information for developing strategies that minimize the particle formation during active regenerations of NOx adsorbers.

Keywords: Diesel engine; Transient operation; NOx adsorber; Active regeneration; EEPS

* Corresponding author. Email: jian@bnl.gov

INTRODUCTION

Epidemiological and laboratory studies have linked exposure to particles less than 2.5 microns in diameter with adverse health effects (Dockery et al. 1993; Pope et al. 1995; Wichmann et al., 2000). Emission from internal combustion vehicles is one of the major sources of sub 2.5 micron particles ($PM_{2.5}$) and it is well-known that diesel engines emit more particle (also called particulate matter, or PM) mass per unit mass of fuel consumed than normal gasoline vehicles. Because of their superior fuel economy, diesel vehicles represent a growing portion of vehicle market world wide. Over 85 percent of the total value of goods in the U.S. is transported by heavy-duty diesel trucks. In Europe, diesel-powered passenger cars currently make up about half of the market share, and are likely to increase in the near future. Future regulations in the U.S. and Europe will reduce diesel PM emissions ten-fold or greater, but it is still important to understand the PM emissions of existing diesel engines and vehicles and their impact on ambient air quality. It is also important to understand the nature of the PM emissions from advanced diesel engines that will likely use diesel particle filters (DPFs) for control.

A number of recent studies have examined the physical characteristics of particle emissions from diesel engines and vehicles. These studies were mostly carried out under steady state engine operation conditions (Holmén and Ayala 2002; Kittelson et al. 1998), and time-resolved studies of diesel particle emissions during transient engine operations were rare (Lehmann et al. 2003; Holmén and Qu 2004; Clark et al. 2005). In the real world, vehicles are operated at a variety of conditions. Diesel engine emissions under transient operating conditions, such as acceleration, deceleration, and change of engine torque, need to be understood for developing realistic particle emission models.

Knowledge of diesel engine emissions under the full spectrum of operating conditions is also required for the development and simulation of DPFs, which are becoming necessary for future diesel vehicles to meet the new, stricter PM emission regulations.

One of the main reasons for the scarcity of diesel particle emission and size distribution data under transient operating conditions is the lack of real-time instruments that are capable of capturing fast changing particle size distributions. Two commercially available instruments, the Electrical Low Pressure Impactor (ELPI, Dekati) and the Scanning Mobility Particle Sizer (SMPS, TSI Inc), have been widely used to measure particle emissions of diesel engines and vehicles. The advantage of the SMPS is its capability of measuring submicron particles with high size resolutions. However, the SMPS measures one particle size at a time. To obtain an entire size distribution, one needs to scan the classifying voltage of the SMPS through a wide dynamic range (Wang and Flagan 1990). As a result, the time resolution of the SMPS is limited to 60 seconds or longer, and thus it cannot capture fast variations of particle size distribution during transient engine operation. Wang et al. (2002) developed a fast response mixing type CPC. When used as the detector in a SMPS system, the Mixing CPC allows size distribution measurements in 1 second. Using a fast SMPS system based on the Mixing CPC, Shah and Cocker (2005) recently reported measurement of transient diesel vehicle emission at a speed of 0.4 HZ. The ELPI measures particle size distributions on the order of seconds by detecting particles of different aerodynamic sizes simultaneously. However, the size resolution of the ELPI is limited (12 stages ranging from 30-10000 nm). While the SMPS and ELPI are based on different size measurement principles, previous measurements during steady state operations have shown that the two

instruments have reasonable agreement in their overlapping size range (Ahlvik et al. 1998; Shi and Harrison 1999).

In this study, a new commercially available instrument, the Engine Exhaust Particle Sizer (EEPS), was tested for measuring diesel engine emissions during transient operation. The EEPS has a good size resolution between 5.6 -560 nm, and is capable of sampling at frequencies up to 10 HZ. Diesel emissions during two types of transient operations were studied. First, particle emissions from a medium-duty engine during the EPA Federal Test Procedure: Heavy-Duty Transient Test (HDTT) cycles were characterized with two diesel fuels. Variations of particle size distributions during the HDTT cycle are presented, and the effects of two fuels on exhaust particle size distribution during transient operations are discussed. We also present an approach to analyze the effect of individual engine parameters on particle emissions. Implications for future strategies to meet pending emissions regulation are discussed. In addition to transient test cycles, transient particle emissions during active regenerations were characterized for a light-duty diesel engine equipped with a NOx adsorber catalyst.. Results of two different active regeneration strategies and the effect of minimum air to fuel ratios on particle emissions are presented.

DIESEL ENGINE PARTICLE EMISSIONS DURING THE FEDERAL TEST PROCEDURE (FTP) HEAVY-DUTY TRANSIENT CYCLES

EXPERIMENT SETUP AND INSTRUMENTATION

The particle size distributions of engine emissions were measured by a new Engine Exhaust Particle Sizer (EEPS) manufactured by TSI Inc (Johnson et al., 2003 and

Johnson et al., 2004). The EEPS is based on the development of the electric aerosol spectrometer (Mirme 1994; Mirme and Tamm 1991; Tammet et al. 2002). Using multiple electrometers as detectors, the EEPS measures particle size from 5.6 to 560 nanometer with a sizing resolution of 16 channels per decade, i.e. total 32 channels. The EEPS reads size distribution at a frequency of 10 HZ, which makes it an ideal instrument to measure diesel engine particle emissions during transient conditions. An impactor is installed at the inlet of the EEPS to remove particles with aerodynamic diameter larger than 1 μm. Particles passing through the impactor are then charged in a unipolar diffusion charger to a predictable charge state. The charged particles subsequently enter an annular space between two cylinders. Under the electrical field between the two cylinders, particles with different mobilities are collected by a series of 22 electrometer rings. The currents from the 22 electrometers do not directly relate to specific particle size channels. Particles that enter the EEPS at the same time are detected at different times, on different electrometers, depending upon size and charge (Johnson et al., 2003). In addition, multiple charging will cause particles of the same size to be detected at different electrometers. A data inversion algorithm accounts for these factors and generates size distribution curves, which are given in 32 size bins that are equally spaced on a logarithmic scale.

A 1999 model year, 5.9L medium-duty diesel engine specially equipped with exhaust gas recirculation (EGR) was used in this study. These engines are most often found in heavy-duty pickup trucks, and are certified for engine emissions like heavy-duty engines, as opposed to having their vehicle emissions certified. The fueling and turbocharger on this engine were modified to allow it to meet the 2004 emissions

standards for NOx. Although this engine was not in a commercial product, its emissions are representative of 2003 model year and later engines found in heavy-duty pickup trucks. A full description of the engine and dynamometer research cell appeared earlier (Kass et al., 2003). A Dyne Systems controller and data acquisition system was used to record data. Engine temperatures, engine speed, torque, power, fuel flow, air flow, and gaseous emissions (CO, CO_2, NOx, and total hydrocarbons (HC)) were recorded. Particle emissions were characterized for two diesel fuels, and the fuel lines were purged between fuels. Raw exhaust was sampled through a 2 m heated (190 °C), stainless steel line to the micro-dilution tunnel. The ejector type dilutor (Kittelson et al. 1998) consisted of an inlet nozzle, an annular nozzle and a mixing chamber. Inside the dilutor, particle-free compressed dilution air was mixed with aerosol sample. A pressure drop at the ejector nozzle ensures homogeneous mixing and a constant dilution ratio. The particle dilution flow was passed through filters and activated carbon to remove particles and hydrocarbons. The two fuels tested were a No. 2 diesel certification fuel with 350 ppm sulfur (Conoco Phillips), and an ultralow sulfur (< 15 ppm sulfur) research fuel prepared by BP Amoco (West et al., 2004, referred to as BP-15 afterwards). For tests with BP-15, only one ejector dilutor was used, and measurements were carried out under different dilution ratios to study the effect of dilution ratio on particle emissions. Particle emissions were significantly higher when Certification Fuel was used, and a second ejector dilutor was added in series to reduce the final particle concentrations within the measurement range of the EEPS.

The Federal Test Procedure (FTP) heavy-duty transient test cycle was used in our emission tests (will be referred as FTP transient cycle afterwards). The FTP transient

cycle was designed by the U.S. EPA for emission testing of heavy-duty on-road engines in the United States. The FTP transient cycle was developed to take into account the duty cycles of a variety of heavy-duty trucks and buses in American cities, including traffic in and around the cities, on roads, and on freeways. The FTP cycle has a running time of 1200 seconds, and consists of four phases: the first is "New York Non Freeway" (NYNF) phase typical of light urban traffic with frequent stops and starts, the second is "Los Angeles Non Freeway" (LANF) phase typical of crowded urban traffic with few stops, the third is a "Los Angeles Freeway" (LAFY) phase simulating freeway traffic in Los Angeles, and the fourth phase repeats the first NYNF phase. The average load factor of the FTP cycle is about 20-25% of the maximum engine horsepower available at a given engine speed. The time series of engine speed and torque are given in Figure 1. During this study, the engine was warmed up prior to each test.

RESULTS AND DISCUSSION (FTP TRANSIENT CYCLE TESTS)

Test to test variation.

The engine speed, torque, and total particle number concentrations during tests of two diesel fuels are shown in Figure 1. For BP-15, five tests with dilution ratio ranging from 18 to 37 were conducted. Only one set of test data is available for Certification Fuel. The total particle number concentration was calculated by integrating particle size distributions measured by the EEPS, and was corrected for dilution (i.e., number of particles per unit volume of exhaust at STP). For better statistics, we averaged the 10 Hz EEPS measurements into 1 second intervals, which is sufficiently fast to capture transient behavior of the engine emission during the FTP cycles. The measured particle size of

diesel emissions can be affected strongly by dilution ratio (Khalek and Kittelson, 2000; Suresh and Johnson, 2001). Low dilution ratio could result in nucleation and condensation of semi-volatile organic compounds and sulfuric acid. Since the BP-15 fuel has very low sulfur content, it is unlikely to form sulfuric acid particles. Figure 1(c) shows the time series of total particle number concentration with dilution ratio ranging from 18 to 37 for tests using BP-15 fuel. The total particle concentrations are nearly identical for different tests, suggesting when BP-15 is used, the effect of dilution ratio on particle number concentration was small over the range tested. For the test using Certification fuel, two dilutors were used in series to reduce the particle concentration within the measurement range of the EEPS. The dilution ratios for the first and second dilutor are 28.4 and 8.5, respectively. Due to the high dilution ratio of the first dilutor, the temperature of the air sample exiting the first dilutor was close to the temperature of the dilution flow. Therefore, we do not expect any change of particle size distributions within the second dilutor. It is worth noting that the dilution ratios used in this study are substantially smaller that those under typical atmospheric conditions. For both fuels, high particle number concentrations were mainly associated with heavy acceleration, high engine speed, and high engine torque. The highest particle number concentrations were 1.7e8/cm^3 and 8e8/cm^3 for BP-15 and Certification Fuel, respectively. Averaged over the entire transient cycle, the number of particles emitted per unit diesel consumed during the test using Certification Fuel was 4.7e12/g-fuel, about three times the average emission rate during BP-15 tests, for the diesel engine tested.

Particle size distribution and emission rate

To analyze engine emissions under different driving characteristics, we divided the FTP transient cycle into four operation modes: acceleration, deceleration, cruise, and idle. The time period of each operation mode is shown in Figure 2. Particle size distributions were averaged over the time period of each operation mode, and the results for both fuels are given in Figure 3. The averaged particle size distributions consist of two particle modes: an ultrafine mode with diameter near 10nm and an Aitken mode with diameter around 60 nm. The averaged size distributions were fitted into two-mode lognormal size distributions:

$$n(D_p) = \sum_{i=1}^{2} \frac{N_i}{\sqrt{2\pi} D_p \ln(\sigma_i)} \exp\left[-\frac{\left(\ln D_p - \ln D_{p,i}\right)^2}{2\ln^2 \sigma_i} \right] \quad (1)$$

where N_i, $D_{p,i}$, and σ_i are the number concentration, geometric mean diameter, and dispersion of each particle mode. The fitted parameters for size distribution averaged over each operation mode are listed in Table 1. For both fuels, particles smaller than 100 nm in diameter made up the majority of the particle population during each operation mode. Except during engine idling, Aitken mode particles dominated the particle total number concentration. For both fuels, the particle number concentrations during "acceleration" and "cruise" periods were significantly higher than those during "deceleration" and "engine idling". The Aitken mode diameter of particle size distribution remained relatively constant among different operation modes when BP-15 was used, whereas for Certification Fuel, the Aitken mode diameter varied from 52 nm to 78 nm. The minimum Aitken mode diameter was observed during “engine idling” and the maximum Aitken mode diameter was observed during "acceleration". While based

on limited tests on a single engine, the above results indicate diesel fuel has strong effects on particle emissions, both in concentration and size, during transient operations. While by no means universal, the significant difference in Aitken mode diameter between the two fuels has broad implications for 2006 and beyond, when all on-road diesel fuel must contain < 15 ppm sulfur. The substitution of the ultra-low sulfur fuel could decrease PM mass emissions, and the changes in particle size could also affect the performance of emissions control devices.

Figure 4 and 5 show the temporal variations of engine parameters and particle size distributions during two typical acceleration and cruise periods. High particle number concentrations were mainly associated with heavy acceleration, high engine speed and torque, as is apparent by comparing the peaks in particle number concentration and engine speed and torque traces. Similar to results shown in Figure 3, the ultrafine mode particles dominated the total particle number concentration during the engine idling. As the engine accelerated from the idle speed (850 rpm, Figure 4 and 5), the ultrafine particle mode declined. At the same time, the concentration of Aitken mode particles increased drastically, which led to significant increase in total particle number concentration. In addition to increased particle number concentrations, Aitken mode diameter of size distribution also varied as the engine accelerated from the idling speed. For tests using Certification Fuel, the Aitken mode diameter first increased to 120 nm, then decreased to the pre-acceleration size of around 60nm, whereas for tests of BP-15, only a moderate increase in mode diameter to 70 nm was observed, followed by a faster decrease back to 50 nm (Figure 4e and 5e). Similar increases in Aitken mode diameter and particle number concentration were also observed during a following engine

acceleration from 1100 rpm (Figure 4, time: 44-57 seconds) for test with Certification Fuel. When BP-15 was used, the increase in particle number concentration during acceleration from 1100 rpm was much less pronounced than that during the initial acceleration from the idle speed, and no increase in Aitken mode diameter was observed. Figures 4b and 4c show that for the test using Certification Fuel, the increase of particle number concentration lasted longer, as evidenced by much broader concentration peaks in the time series. The main differences between the two fuels is the low sulfur content of BP-15, and the deep hydrotreatment of BP-15 leads to lower aromatics, which are thought to be soot precursor molecules. BP-15 also has fewer fuel residuals, such as asphaltenes, which can form condensation nuclei (Rhead and Hardy 2003; Tancell et al. 1995). As the Aitken mode particles are primarily soot, and the ultrafine fraction is typically condensables such as heavy fuel and/or lubricant molecules (Jung et al. 2003), we expect a lower particle emission rate when BP-15 is used. The larger Aitken mode diameter observed during the tests using Certification Fuel may indicate an enhancement in the rich zone of the flame during these periods, due to the lower cetane number and slower, or retarded, ignition of the Certification Fuel. The extra time with depleted oxygen may therefore allow for increased growth on/with soot precursor compounds such as Polycyclic Aromatic Hydrocarbons (PAHs) which are higher in the Certification Fuel. Additionally, the higher cetane of the BP-15 fuel will generally advance the ignition timing leading to less particle formation (Heywood, 1988). At a constant engine speed, an increase in engine torque led to increases in both particle number concentration and Aitken mode diameter when Certification Fuel was used, whereas the Aitken mode diameter remained the same for tests using BP-15. Growth of Aitken mode diameter

during engine accelerations and increases of engine torque explains the larger mode diameter of particle size distributions averaged over "acceleration" and "cruise" operation modes when Certification Fuel was used (Figure 3). Variations of particle size distributions described above were typical throughout the FTP transient cycle. The analyses of FTP test results show high emission rates are often associated with heavy accelerations, and diesel fuel has strong effects on both particle size and concentration of diesel emissions during transient operations. Furthermore, the fuel effects on emissions are quite different for different driving characteristics. Note the above results are based on limited FTP tests using one diesel engine. It will be interesting to see if similar fuel effects on transient emissions can be observed for diesel engines in other classes. Future studies will also include the fuel effects on transient emissions under different dilution ratios and conditions.

In addition to particle number concentrations, engine emission rates (particle number or volume emitted per second) and emission (particle number or volume) per unit fuel consumed were studied. The emission rate (number or volume) is the product of particle concentration (number or volume) and exhaust flow rate, which was derived from the measured intake air flow rate and the engine fuel flow rate. The fuel flow rate was measured with a Max Machinery fuel flow meter. Figure 6 shows the emission rates (both number and volume), and emission per unit fuel averaged over the four different operation modes and three phases of the FTP transient cycle. It is important to note that the volume emission rates are calculated assuming spherical particles, which is not a good assumption for particles emitted by diesel engines. As a result, there could be substantial uncertainties associated with the volume emission rates presented in Figure 6.

Between the two fuels tested, the emission rates (both number and volume based) were consistently higher for Certification Fuel during each operation mode and phase. As a result of both high particle concentration and exhaust flow rate, the emission rates during "acceleration" and "cruise" modes were higher than those during "deceleration" and "idle" modes for both fuels. Figure 6 shows the large differences among emission rates averaged over different phases. LAFY, which has a long period of high speed cruise, had the highest emission rate, while the NYNF had the lowest emission rate due to the long period of engine idling. The differences among different phases were significantly reduced when the emission rate was normalized by the amount of diesel fuel consumed. The variation in number emission per unit diesel consumed was about 40% (1.4e12-1.9e12/gm) and 30% (4.3e12-5.6e12/gm) for BP-15 and Certification Fuel, respectively. For volume emission per unit diesel consumed, the variation was 40% (2.0e8-2.8e8 μm^3/gm) for BP-15 and 75% (1.2e9-2.1e9 μm^3/gm) for Certification Fuel.

Effect of engine parameter on particle concentration and emission rate

In this section we present an approach to analyze the effects of individual engine parameter on particle concentration during transient operations, and the approach is applied to the FTP test data described above. To investigate the effect of each engine parameter on the particle number concentration and emission rate, the particle number concentration and number emission rate were fitted to engine parameters through multiple linear regression. Prior to fittings, the particle number concentration and emission rate of each fuel type, and engine parameters were normalized using the following equation:

$$\tilde{X} = \frac{X - \overline{X}}{\sigma_X} \quad (2)$$

where $\overline{X}$ and σ_X are the mean and standard deviation of the variable X. X represents either the particle number concentration or engine parameters. Through linear regression, we hypothesize that the normalized particle number concentration $\tilde{N}$ can be approximated by a linear function of following normalized engine parameters:

$$\tilde{N} \approx a_0 + a_1\tilde{v} + a_2\widetilde{\frac{dv}{dt}} + a_3\widetilde{Tq} + a_4\widetilde{\frac{dTq}{dt}} \quad (3)$$

where a_i (i=0-4) are the regression coefficients, v the engine speed, Tq the engine torque, and $\frac{dv}{dt}$ and $\frac{dTq}{dt}$ the engine acceleration and the change rate of engine torque, respectively. The linear regressions of the particle number concentration were performed on the above four engine parameters with data from "Acceleration", "Deceleration", and "Cruise" operation modes. The resulting regression coefficient of each engine parameter and the correlation of the regression are listed in Table 2. The linear regression was not performed for data during the "Idle" operation mode due to nearly constant engine speed and torque. The selection of the fitting parameters is based on both particle emissions observed during the FTP tests and statistical approaches. In addition to engine speed and torque (v, Tq), high particle concentrations were observed during heavy accelerations ($\frac{dv}{dt}$) for both fuels tested. Figure 5 shows rapid increases of engine torque ($\frac{dTq}{dt}$) often lead to high particle concentrations when Certification fuel is used. Engine power, one of the obvious choices, is not used in the regression because when engine power is included in addition to the above four engine parameters, linear regressions show no appreciable

difference in the resulting correlation coefficients. Furthermore, when one of the four parameters is replaced by the engine power, linear regressions often result in lower correlations. Therefore, the four parameters are appropriate choices for linear regression analyses, and the high correlation coefficients (as shown later) indicate linear combinations of the four parameters capture most of the variations in transient particle emissions for the diesel engine studied. The effects of individual engine parameter on transient particle emissions may depend on engine technology or architecture. Different sets of engine parameters may be more appropriate for transient emissions of other engines, which will be topics of future studies.

Table 2 shows that linear regressions yielded high correlations during each operation mode, especially for data with BP-15. The high correlations indicate most of the observed variations in particle number concentration N can be explained by variations of the four engine parameters. It is worth noting for data of different operation modes, the particle number concentration and engine parameters were normalized using the mean ($\overline{X}$) and standard deviation (σ_X) of the entire FTP transient cycle. Therefore, regression coefficients (a_i, i=0-4) among different operation modes are directly comparable for each fuel. When BP-15 was used, the regression coefficient of $\frac{\widetilde{dTq}}{dt}$ was much smaller than coefficients of other engine parameters for each operation mode. The absolute value of the regression coefficient of $\frac{\widetilde{dTq}}{dt}$ was less than 0.1, suggesting that the particle number concentration was not a strong function of $\frac{dTq}{dt}$ during tests using BP-15. After $\frac{\widetilde{dTq}}{dt}$ was removed as a variable, the linear regression of $\widetilde{N}$ was performed on the remaining

three engine parameters, and the resulting correlation and regression coefficients were nearly identical. The insensitivity of particle number concentration to $\widetilde{\frac{dTq}{dt}}$ is further supported by Figure 7d, which shows little variation in particle number concentrations averaged over different $\frac{dTq}{dt}$ ranges during BP-15 tests. The regression coefficients of $\tilde{v}$, $\widetilde{Tq}$, and $\widetilde{\frac{dv}{dt}}$ were all positive, indicating high particle number concentrations were mainly associated with heavy acceleration, high engine speed, and torque. The regression coefficient of $\widetilde{\frac{dv}{dt}}$ during "acceleration" mode (0.49) was substantially larger than those during "deceleration" (0.13) or "cruise" mode (0.16), which suggests $\widetilde{\frac{dv}{dt}}$ had a strong effect on particle number concentration during heavy acceleration, and less impact on particle number concentration during "cruise" and "deceleration" modes.

Similar to BP-15, the particle number concentration during tests using Certification Fuel increased with increasing $\frac{dv}{dt}$ and Tq, as evidenced by the positive regression coefficients listed in Table 2 and results shown in Figure 7b and 7c. The effects of v and $\frac{dTq}{dt}$ on particle number concentration were different for tests using Certification Diesel and BP-15. The particle number concentration increased with increasing $\frac{dTq}{dt}$ when Certification Fuel was used. On the other hand, the small coefficients derived from the linear regression suggest particle number concentration was insensitive to engine speed for Certification Fuel. This conclusion is supported by the

result shown in Figure 7a and the fact that the new linear regression yielded similar correlation and regression coefficients after v was removed as a fitting variable. Comparison of coefficients of $\frac{dv}{dt}$ between the two fuels indicates engine acceleration has a larger impact on particle number concentration for Certification Fuel than BP-15.

Because the overall flux of particles from an engine is more critical to engine emission control, the correlation and regression coefficients from the linear regression of number emission rate are listed in table 3. The correlation of the linear regression was higher than 0.8 except for the "deceleration" mode when Certification Fuel was used. The engine particle number emission rate is the product of the particle number concentration and the exhaust flow rate. The correlations between engine exhaust flow rate and engine speed and torque were 0.70 and 0.69, respectively. As both particle number concentration and engine exhaust flow rate increased with increasing engine speed and torque, it is expected that the engine emission rate is a strong function of engine speed and torque. For tests using BP-15, the regression coefficients derived from the linear regression indicate the majority of the variation in engine emission rates can be explained by variations in engine speed and torque, and the engine particle number emissions were not strong functions of $\frac{dv}{dt}$ and $\frac{dTq}{dt}$. Combining data from the three operation modes, linear regression of the particle number emission rate on engine speed and torque yielded a high correlation of 0.87, suggesting the particle number emission rate can be well explained from engine speed and torque for the BP-15 fuel. While it is well-known that the number of particles emitted increases with engine speed and load, the lack of dependence on both $\frac{dv}{dt}$ and $\frac{dTq}{dt}$ is surprising, since the assumption has

always been that rapid transients are responsible for the majority of particle emissions. In contrast, for Certification Fuel, the engine speed and torque alone were not sufficient to explain all the variations in particle emission rate. Among all four engine parameters, only the effect of $\frac{dTq}{dt}$ on emission rate was negligible. After removing $\frac{dTq}{dt}$ as a variable, linear regression of number emission rate yielded similar correlation and coefficients for remaining three engine parameters. As the particle number concentration was insensitive to engine speed during the Certification Fuel test, the strong effect of engine speed on particle emission rate was a result of strong correlation between exhaust flow rate and engine speed. The difference in dependence of engine emissions on engine parameters may be related to the difference between the cetane numbers of the two fuels. The cetane number of BP-15 is higher than that of Certification fuel. The straight substitution of BP-15 effectively shortens the ignition delay of the fuel. This property could lead to less particle formation during periods of high fuel demand such as acceleration or torque increase, when local concentrations in the cylinder can be fuel-rich. Once the turbocharger has spooled up to match the new engine speed, or exhaust flow, a leaner air-fuel ratio is achieved and the particle formation decreases in a corresponding manner.

Whereas based on limited tests, the above analyses indicate for different diesel fuels, individual engine parameters have different effects on transient particle emission and its size distribution. In particular, the particle number emission rate is a strong function of engine acceleration when Certification Fuel is used, but is insensitive to engine acceleration for tests using BP-15 fuel. The effect of individual engine parameters may be different for different diesel engines. Since the above results are based on tests

on one engine, future studies will include more tests to verify the above findings, and study the effects of engine parameters on transient emissions for other representative diesel engines.

DIESEL ENGINE EMISSION DURING NO_X ADSORBER ACTIVE REGENERATION

NO_X ADSORBER ACTIVE REGENERATION AND EXPERIMENTAL SETUP

NOx adsorber regeneration

As regulations on diesel engine NOx and particulate emissions become more strict, future diesel engines will likely require efficient aftertreatment to meet the new emission regulations. One aftertreatment technology being researched is the NOx adsorber or Lean NOx Trap, which reduces NOx from diesel exhaust. The details of NOx adsorber operation were given in West et al (2004). The operation of a NOx adsorber proceeds through a series of reaction steps involving oxidation, storage, and reduction functions. In a fuel lean (oxygen-rich) environment, typical of diesel engine exhaust, NO is oxidized by the catalyst to NO_2, which is further oxidized to nitrate through a surface-catalyzed reaction. The nitrates produced are stored on the catalyst surface; therefore, the nitrate storage sites on the catalyst need to be regenerated periodically in order to adsorb more NOx. The "recovery" process is called active regeneration. During active engine-based regeneration, the engine is operated for a short period under fuel rich (oxygen-depleted) conditions, and stored NOx is released and reduced to N_2 by the catalyst. The transitions of the engine between the fuel-lean and fuel-rich operation can cause formation of particulate (West et al, 2004; Witze et al,

2004), and such rapid changes in particle emission can be characterized using the fast EEPS.

Experimental setup

A Mercedes OM668 1.7 liter common-rail diesel engine coupled to a motoring DC dynamometer was used in this study. The engine was a 1999 model used in the Mercedes A170 automobile in Europe. The factory engine control module was replaced with a rapid development engine controller based on a dSpace® MicroAutoBox. This rapid development system (RDS) provides complete control over all engine electronics, including timing, duration, and number of fuel injection events, intake throttle, etc. A full description of the engine and dynamometer research cell, and the two regeneration strategies studied here was given in West et al (2004). For both regeneration strategies, the regeneration window lasts 10 seconds and employs intake throttling to lower exhaust oxygen concentration. Five seconds into the regeneration process, excess fueling was used to transition to fuel-rich operation. The duration of excess fueling was 3 seconds. For the first strategy tested, "Delayed Extended Main" (DEM), the main injection duration was extended for three seconds to achieve fuel-rich conditions, and injection was retarded a few crank angle degrees to reduce the torque increase associated with excess fueling. The second strategy examined here, "Post80", uses a throttle strategy identical to that of the DEM strategy, but excess fuel injection occurs after the main injection, 80 degrees after top dead center (ATDC). The pilot injection, the small pre-injection event used to quiet the diesel "clatter", was disabled during Post80. DEM and Post 80 are two major strategies that are being explored for NOx adsorber regenerations.

Between the two strategies, the DEM has higher NOx adsorber regeneration efficiencies than Post80 (West et al., 2004).

Each of these NOx adsorber active regeneration strategies causes a similar, rapid decrease in air-to-fuel ratio (AFR), but in very different ways. The DEM strategy consumes excess oxygen in the combustion process; the Post80 strategy consumes oxygen later in the power stroke. Since the entire active regeneration process last only 10 seconds, the fast changing particle emissions are best characterized using an EEPS, which is capable of high time resolution measurements. The data on particle emissions during active regeneration are important for formulating low particle emission regeneration strategies, as well as designing and simulating diesel particulate filters for the exhaust system involving the regeneration processes.

The setup of the NOx regeneration experiment is presented in Figure 8. The exhaust coming out of the NOx adsorber was transported through a 3-meter heated line, which was maintained at a minimum temperature of 190 °C. The exhaust delivered through the heated line was fed into two ejector dilutors that were operated in series. The dilution ratio after the two dilutors was maintained at 650:1. The dilution flow was passed through filter, trap and active carbon to remove hydrocarbon and particles. The RH of the dilution flow was below 5%. It is worth pointing out that the light-duty engine used in the NOx adsorber study was not equipped with a Diesel Particulate Filter (DPF). Vehicle particulate emissions have been declining for many years and upcoming stringent regulations around the world will almost certainly require vehicles to use a DPF to remove PM from exhaust. The focus of the study is to characterize the particles generated with the different NOx adsorber regeneration strategies. The size,

concentration, and other characteristics of the particles entering a downstream DPF have important implications for the capacity and performance of the DPF.

RESULTS AND DISCUSSION (NO_X ADSORBER ACTIVE REGENERATION)

For each regeneration strategy, active regenerations were repeated once per minute. Figure 9 gives the variation of particle number concentrations as a function of time during repeated DEM regenerations. The particle number concentrations were calculated by integrating the size distributions measured by EEPS, and were corrected for dilution. The particle number concentration during active regenerations was very reproducible, as evidenced by nearly identical particle number concentrations during different tests. As pointed out earlier, the diesel engine studied here is not equipped with a DPF. As a result, the particle concentrations shown here are much higher than emissions from future realistic diesel vehicles.

Figure 10 presents the air flow, air to fuel flow ratio, and image plots of particle size distributions during the DEM and Post80 regenerations. The minimum air-to-fuel ratio (AFR) for both regenerations was maintained at a fuel-rich 13:1 (The stoichiometric AFR value is 14.7:1). The particle size distributions were averaged over repeated tests. During DEM regenerations, the time series of particle number concentration showed a single peak, while during Post80 regenerations, two concentration peaks and a valley between the peaks were observed. The second-by-second particle size distributions measured by EEPS were fitted into lognormal distributions, and the Aitken mode concentration and diameter are plotted as functions of time in Figure 11. Results from regeneration events under less fuel-rich conditions, AFR= 14:1, are also given. As

apparent from Figure 11c and 11d, the effects of the two regeneration strategies on particle emission were quite different. During DEM regenerations, the diesel particle number concentration started to increase as the air flow was reduced. The number concentration reached a maximum of 4.8e8/cm^3 when air to fuel ratio dropped to the minimum of 13 during the excess fueling. The particle number concentration then decreased to the pre-regeneration level as the AFR recovered to normal fuel-lean conditions. When the minimum AFR was 13:1, the particle number concentration averaged during the DEM regeneration was 2.1e8/cm^3, a factor of 2.9 greater than the pre-regeneration level (5.4e7/cm^3). In addition to increases in particle number concentration, the particle mode diameter during DEM regeneration doubled from 60 nm to 120 nm. For the Post80 regeneration strategy, we observed quite different effects on particle emissions. Like DEM, the particle number concentration first increased as the air flow was reduced. Once the excess fueling started, the particle number concentration began to decrease, producing the first concentration peak. The particle number concentration decreased to a minimum of 3.2e7/cm^3, which was even *below* the pre-regeneration level of 4.5e7/cm^3, as the AFR was at the minimum of 13:1. The particle number concentration then increased from the minimum to the second peak as the excess fueling ended, then decreased to pre-regeneration concentrations as the air flow recovered. For Post80 regenerations with a minimum air to fuel ratio of 13, the particle number concentration averaged regenerations only increased slightly from the pre-regeneration level of 4.5e7/cm^3 to 5.0e7/cm^3. The particle mode diameter remained relatively constant around 60 nm throughout the Post80 regenerations. Between the two regeneration strategies, Post80 had a much smaller emission rate than DEM. Averaged

over the Post80 regenerations with a minimum AFR of 13, the particle volume concentration only slightly increased from 1.9e4 $\mu m^3/cm^3$ to 2.0e4 $\mu m^3/cm^3$. In contrast, particle volume concentration averaged over DEM regeneration increased by a factor of 16 from pre-regeneration level of 2.6e4 $\mu m^3/cm^3$ to 4.4e5 $\mu m^3/cm^3$, which was due to a combination of high particle number concentration and larger particle diameter during the DEM regenerations. Comparison of the particle number concentrations and mode diameters at different minimum AFR values (13:1 and 14:1) indicates that AFR had only a small effect on particle size and concentration for both regeneration strategies. The higher particle emission during DEM regeneration could be explained by the following: the additional fuel added during combustion initiated by the pilot fuel injection has the effect of increasing the rich, soot-producing zones of the flame, leading to increased particle growth as well as concentration. Witze et al (2005) speculate that the *decrease* in particle number emissions during Post80 may be caused by the lack of pilot fuel injection. Because there is no existing flame as the main fuel injection proceeds, there is no addition of fuel to a rich, sooting zone. The rapid increase in particle emissions at the end of Post80 may be due to the excess fuel interfering with the normal oxidation processes of the soot, or combustion of the excess fuel.

The emissions control engineering and environmental implications of this research are important. In 2009 (light-duty vehicles) and 2010 (heavy-duty vehicles), additional restrictions on mobile source emissions will take full effect. These new regulations will likely necessitate NOx adsorber catalysts or some other form of catalytic NOx emissions control. The EEPS, and the data analysis presented in this study, can be invaluable for developing regeneration strategies that minimize excessive particle

formation and work in concert with diesel particulate filters (DPFs) for overall emissions reduction. Furthermore, by incorporating size-resolved PM emissions as a function of engine and emissions control operation, it may be possible to improve the ability of mobile source emissions models to predict impacts of diesel particle emissions on ambient $PM_{2.5}$.

CONCLUSIONS

The diesel engine emissions during transient operations were studied using the newly developed EEPS. Particles emitted by a 1999 model year, medium-duty diesel engine during engine FTP transient cycles were characterized for different diesel fuels: Certification Fuel and BP-15. For both fuels tested, high particle number concentration and emission rates were associated with heavy acceleration, high speed, and high torque. Averaged over the FTP transient cycle, the particle number concentration during a test using Certification Fuel was 1.2e8/cm^3, about four times the particle number concentration during BP-15 tests. For both fuels, the particle size distributions observed during the FTP transient cycles consisted of two modes: one ultrafine mode with modal diameter around 10 nm and an Aitken mode with modal diameter ranging from 50 nm to 80 nm. When Certification Fuel was used, both the particle number concentration and the Aitken mode diameter increased during engine accelerations and increases in engine torque. In contrast, for BP-15, only a moderate increase in Aitken mode diameter was observed when the engine accelerated from the idle speed (850 rpm). Engine acceleration from higher engine speeds and increases of torque resulted in higher particle number concentrations whereas the Aitken mode diameter remained unchanged for BP-

15. The particle number emission per unit diesel fuel was relatively constant among the three phases of the FTP transient cycle. The variations in number emission per unit diesel consumed were about 40% (1.4e12-1.9e12/gm) and 30% (4.3e12-5.6e12/gm) when BP-15 and Certification Fuel were tested, respectively. The effect of each engine parameter on particle emission was studied through linear regression of particle number concentration and number emission rate on four engine parameters. For BP-15, it was found the particle number emission rate can be well predicted from engine speed and torque. When Certification Fuel was used, the engine acceleration ($\frac{dv}{dt}$) strongly affected the particle number emission rate in addition to the engine speed and torque. It is important to note that the above interesting findings are based on limited tests on one engine. Future studies will include additional tests to verify these results, and study the effects of diesel fuel and engine parameters on transient particle emissions for other representative diesel engines. Nonetheless, the research described here has broad implications for both engine and emissions control development as well as mobile source effects on air quality. As more strict emissions regulations take effect, sources and characteristics of ambient fine particulate matter, particularly on urban roadways, will be changing. The combination of the EEPS and data analysis techniques demonstrated here may greatly increase the effectiveness of emissions control strategies. The unprecedented ability to measure particle size distributions during transient operations, as well as the development of data models for a given engine and fuel combination, promises to assist in calibration of strategies for both engine operation and emissions control. Mobile source models, which characterize emissions as a function of vehicle operation, traffic,

and road conditions, could potentially utilize the data analysis methods described here to improve their treatment of particle emissions.

The particle size distributions during active regenerations of a diesel NOx adsorber catalyst were also characterized using the EEPS. Two regeneration strategies, Delayed Extended Main (DEM) and Post80, were studied. During the DEM regenerations, substantial increases in particle number concentration and particle mode diameter were observed. As a result, for DEM regenerations with a minimum air to fuel flow ratio of 13:1, the particle volume concentration averaged over the regenerations reached 4.4e5 $\mu m^3/cm^3$, a factor of 16 of the pre-regeneration level of 2.6e4 $\mu m^3/cm^3$. For the Post80 regenerations, intake throttle (reducing the air flow) and increasing the fuel injection had opposite effects on particle number concentrations, which resulted in two peaks in the time series of particle number concentration during regenerations. Little variation in particle mode diameter was observed during Post80 regenerations. During Post80 regenerations with a minimum AFR of 13:1, the average particle volume concentration only increased slightly from the pre-regeneration level of 1.9e4 $\mu m^3/cm^3$ to 2.0e4 $\mu m^3/cm^3$. It was also found that the minimum AFR reached during regenerations had little effect on particle number concentration and mode diameter for both regeneration strategies. Between the two regeneration strategies studied here, Post80 had much lower particle emission rates than DEM regenerations.

ACKNOWLEDGMENTS

This work was supported by the U.S. Department of Energy (DOE), Office of FreedomCAR and Vehicle Technology. The authors gratefully acknowledge the support

and guidance of Dr. James Eberhardt at DOE, and his encouragement for inter-laboratory cooperative research. The authors also acknowledge the support of Jian Wang through the Goldhaber distinguished fellowship of Brookhaven National Laboratory. Grateful acknowledgment is also due to Jeff Chambers and Eric Nafziger of ORNL for their outstanding technical support in the laboratory, and Tim Johnson and Jeremy Kolb of TSI Inc for their assistance in operation of the EEPS.

ORNL is a multiprogram science and technology laboratory managed for the U.S. Department of Energy by UT-Battelle, LLC. ORNL is a program of the Department of Energy's Oak Ridge Field Office.

Disclaimer

REFERENCE

Ahlvik, P., Ntziachristos, L., Keskinen, J. (1998) *SAE Tech. Pap. Ser.* NO. 980410.

Dockery, D. W., Pope, C. A., Xu, X. P., Spengler, J. D., Ware, J. H., Fay, M. E., Ferris, B. G., Speizer, F. G. (1993). An Association between Air-pollution and Mortality in 6 United States Cities, *New England Journal of Medicine,* 329 (24): 1753-1759.

Heywood, J. B. (1988). Internal Combustion Engine Fundamentals. McGraw-Hill, New York, 1988.

Holmen, B. A., Ayala, A. (2002). Ultrafine PM emissions from natural gas, oxidation-catalyst diesel, and particle-trap diesel heavy-duty transit buses, *Environmental Science and Technology*, 36 (23): 5041-5050.

Holmen, B. A., Qu, Y. G. (2004). Uncertainty in particle number modal analysis during transient operation of compressed natural gas, diesel, and trap-equipped diesel transit buses, *Environmental Science and Technology,* 38 (8): 2413-2423.

Johnson, T., Caldow, R., Pöcher, A. (2003). An Engine Exhaust Particle Sizer™ Spectrometer for Transient Emission Particle Measurements, *7th ETH Conference on Combustion Generated Particles, Zürich, Switzerland*, A117.

Johnson, T., Caldow, R., Pocher, A., Mirme, A., Kittelson, D. B. (2004) A New Electrical Mobility Particle Sizer Spectrometer for Engine Exhaust Particle Measurements, *SAE Tech. Pap. Ser.*, No. 2004-01-1341.

Jung, H., Kittelson, D.B., and Zachariah, M. R., (2003). "The Influence of Engine Lubricating Oil on Diesel Nanoparticle Emissions and Kinetics of Oxidation" Society of Automotive Engineers Technical Series 2003-01-3179.

Kass, M. D., Thomas, J. F., Lewis, S. A., Storey, J. M., Domingo, N., Graves, R. L., and Panov, A. (2003). Selective Catalytic Reduction of NOx Emissions From a 5.9 Liter Diesel Engine Using Ethanol as a Reductant, *SAE Tech. Pap. Ser.*, No. 2003-01-3244.

Khalek, I., Kittelson, D. B., and Brear, F. (2001). Nanoparticle Growth During Dilution and Cooling of Diesel Exhaust: Experimental Investigation and Theoretical Assessment. *SAE Tech. Pap. Ser.*, No. 2000-01-0515.

Kittleson, D. B., Abdul-Khalek, I. S., Graskow, B. R., Brear, F., Wei, Q. (1998). Diesel Exhaust Particle Size: Measurement Issues and Trends. *SAE Tech. Pap. Ser.*, No. 980525.

Lehmann, U., Mohr, M., Schweizer, T., Rutter, J. (2003). Number size distribution of particulate emissions of heavy-duty engines in real world test cycles, *Atmospheric Environment* 37 (37): 5247-5259.

Mirme, A. A. (1994). Electric aerosol spectrometry, PhD Thesis, Tartu University.

Mirme, A., Tamm, E. (1991). Comparison of Sequential and Parallel Measurement Principles in Aerosol Spectrometry, *Journal of Aerosol Science*, 22: S331-S334.

Pope, C. A., Thun, M. J., Namboodiri, M. M., Dockery, D. W., Evans, J. S., Speizer, F. E., Heath, C. W. (1995). Particulate Air-Pollution as a Predictor of Mortality in a Prospective-study of US Adults, *American Journal of Respiratory and Critical Care Medicine*, 151 (3): 669-674.

Rhead, M., and Hardy, S., (2003). "The Sources of polycyclic aromatic compounds in diesel engine emissions," Fuel, Vol. 82, pp. 385-393.

Shah, S. D. and Cocker, D. R. (2005). A fast scanning mobility particle spectrometer for monitoring transient particle size distributions. *Aerosol Science and Technology*, 39 (6) 519-526.

Shi, J. P., Harrison, R. M. (1999). Investigation of ultrafine particle formation during diesel exhaust dilution, *Environmental Science and Technology*, 33 (21): 3730-3736.

Sluder, C.S., Wagner, R. M., Storey, J. M. E., and S. A. Lewis, (2005). "Implications of Particulate and Precursor Compounds Formed During High-Efficiency Clean Combustion in a Diesel Engine." Society of Automotive Engineers Technical Series 2005-01-3844.

Suresh, A. and Johnson, J. H. (2001). A Study of the Dilution Effects on Particle Size Measurement From a Heavy-Duty Diesel Engine With EGR. *SAE Tech. Pap. Ser.*, No. 2001-01-0220.

Tammet, H., Mirme, A., Tamm, E. (2002). Electrical aerosol spectrometer of Tartu University, *Atmospheric Research*, 62 (3-4): 315-324.

Tancell, P., Rhead, M., Pemberton, R., and Braven, J., (1995), "Survival of Polycyclic Aromatic Hydrocarbons during Diesel Combustion," Environmental Science and Technology, Vol. 29, pp. 2871-2876.

Wang, J., McNeill, V.F., Collins, D. R., and Flagan, R. C. (2002). Fast mixing condensation nucleus counter: Application to rapid scanning differential mobility analyzer measurements. *Aerosol Scicence and Technology*, 36 (6), 678-689

Wang, S. C., and Flagan, R. C. (1990). Scanning Electrical Mobility Spectrometer, *Aerosol Science and Technology*, 13: 230-240.

West, B., Huff, S., Parks, J., Lewis, S., Choi, J. S., Partridge, W., and Storey, J. (2004). Assessing Reductant Chemistry During In-Cylinder Regeneration of Diesel Lean NOx Traps. *SAE Tech. Pap. Ser.*, No. 2004-01-3023.

Wichmann, H.-E., Spix, C., Tuch, T., Wölke, G., Peters, A., Heinrich, J., Kreyling, W. G., Heyder, J., (2000). Daily mortality and fine and ultrafine particles in Erfurt, Germany. Part I: role of particle number and particle mass. *Health Effects Institute Report No. 98*

Witze, P.O., Huff, S.P., Storey, .M.E., and West, B.H., (2005). "Time-Resolved Laser-Induced Incandescence Measurements of Particulate Emissions During Enrichment for Diesel Lean NOx Trap Regeneration", Society of Automotive Engineers Technical Series 2005-01-0186.

Table 1: Mode diameter, concentration, and dispersion of particle size distributions averaged over each engine operation mode. Size distributions were fitted to a two-mode lognormal distribution.

Fitted parameter		BP -15				Certification Fuel			
		Accele.	Decele.	Cruise	Idle	Accele.	Decele.	Cruise	Idle
Ultrafine	N_1 (cm^{-3})	6.6E+06	3.2E+06	7.6E+06	8.5E+06	4.4E+07	1.5E+07	2.5E+07	6.9E+07
	$D_{p,1}$ (nm)	11.0	10.7	18.3	8.5	4.9	6.2	3.8	7.1
	σ_1	2.3	2.2	1.9	1.7	1.8	1.9	3.8	1.6
Aitken	N_2 (cm^{-3})	4.0E+07	1.1E+07	3.7E+07	2.8E+06	2.9E+08	5.2E+07	1.5E+08	2.5E+06
	$D_{p,2}$ (nm)	56	49	50	50	78	76	60	52
	σ_2	1.6	1.6	1.6	1.5	1.6	1.7	1.6	2.2

Table 2. Correlations and regression coefficients derived through linear regression of particle number concentration to engine parameters. Results are given for each operation mode for tests with both fuels. The linear regression of particle number concentrations from BP-15 test was also performed on *v*, *dv/dt*, and *Tq*, and the results are given in parenthesis. For tests using Certification Fuel, numbers in parenthesis are results of linear regression of particle number concentration on *dv/dt*, *Tq*, and *dTq/dt* only.

N fitting results	BP-15			Certification Fuel		
	Acceleration	Deceleration	Cruise	Acceleration	Deceleration	Cruise
R	0.81, (0.81)	0.86, (0.86)	0.86, (0.85)	0.78, (0.78)	0.71, (0.71)	0.82, (0.81)
a0	-0.31, (-0.31)	-0.39, (-0.40)	-0.85, (-0.85)	0.09, (0.07)	-0.07, (-0.06)	0.10, (-0.01)
a1 (v)	0.42, (0.42)	0.61, (0.61)	1.04, (1.04)	-0.18, (N/A)	0.07, (N/A)	-0.10, (N/A)
a2 (dv/dt)	0.48, (0.49)	0.14, (0.13)	0.18, (0.16)	0.72, (0.71)	0.26, (0.26)	0.30, (0.30)
a3 (Tq)	0.52, (0.53)	0.49, (0.49)	0.70, (0.70)	0.72, (0.68)	0.57, (0.57)	0.48, (0.48)
a4 (dTq/dt)	0.04, (N/A)	-0.01, (N/A)	-0.08, (N/A)	0.40, (0.39)	0.14, (0.14)	0.33, (0.33)

Table 3. Correlations and regression coefficients derived through linear regressions of number emission rate to engine parameters. Results are given for each operation mode for tests with both fuels. The linear regression of particle number concentrations from BP-15 test was also performed on *v* and *Tq*, and the results are given in parenthesis. For tests using Certification Fuel, numbers in parenthesis are results of linear regression of number emission rate to *v*, *dv/dt*, and *Tq*.

Emission Rate fitting Results	BP-15				Certification Fuel		
	Acceleration	Deceleration	Cruise	all	Acceleration	Deceleration	Cruise
R	0.83, (0.81)	0.88, (0.87)	0.93, (0.91)	0.87	0.86, (0.84)	0.78, (0.77)	0.87, (0.86)
a0	-0.29, (-0.09)	-0.31, (-0.42)	-1.06, (-1.05)	-0.43	-0.09, (-0.10)	-0.11, (-0.11)	-0.49, (-0.50)
a1 (v)	0.84, (0.84)	0.65, (0.66)	1.31, (1.30)	0.80	0.61, (0.61)	0.34, (0.34)	0.62, (0.63)
a2 (dv/dt)	0.18, (N/A)	0.10, (N/A)	0.20, (N/A)	N/A	0.37, (0.41)	0.24, (0.25)	0.34, (0.38)
a3 (Tq)	0.37, (0.33)	0.45, (0.42)	0.78, (0.78)	0.65	0.62, (0.63)	0.52, (0.52)	0.76, (0.77)
a4 (dTq/dt)	-0.04, (N/A)	-0.05, (N/A)	-0.15, (N/A)	N/A	0.17, (N/A)	0.06, (N/A)	0.16, (N/A)

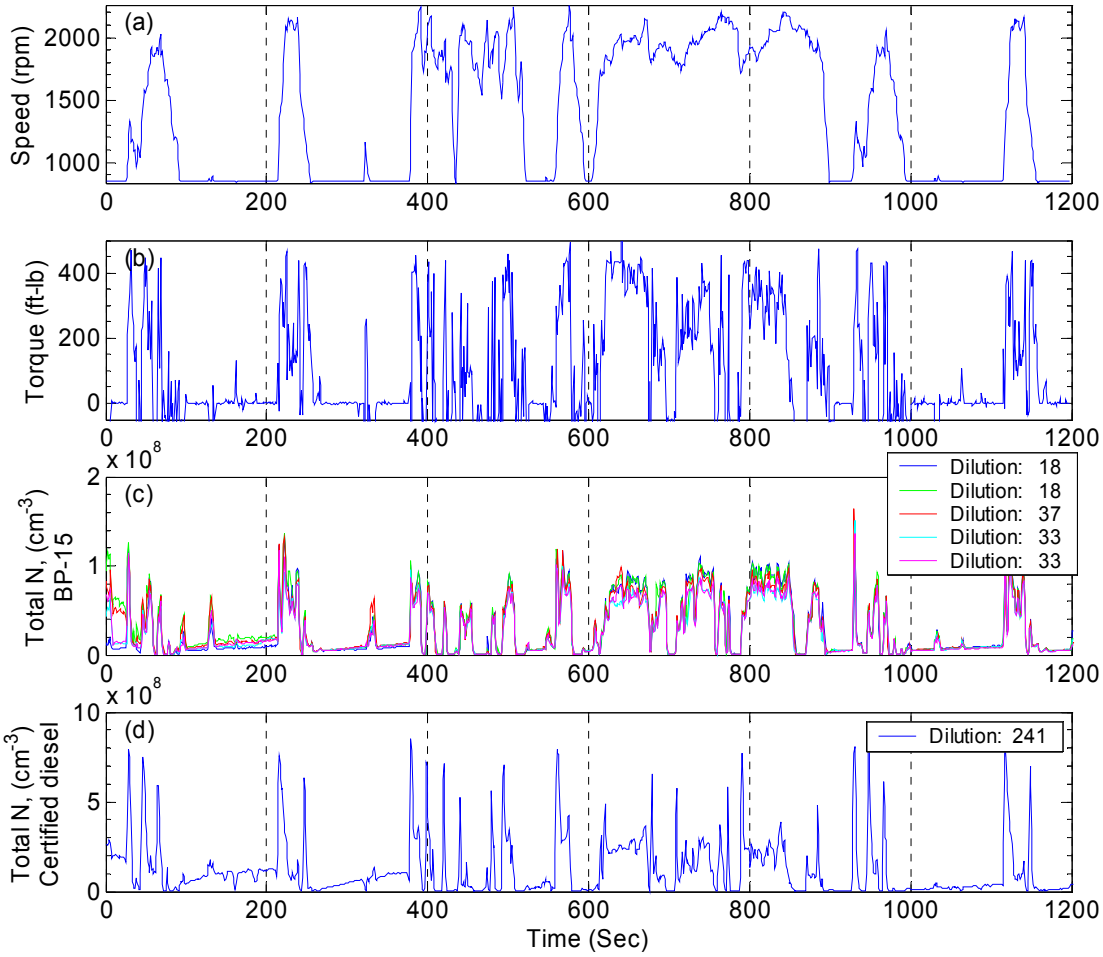

Figure 1: Time series of engine parameters and particle number concentrations during FTP transient test cycles. (a) Engine speed. (b) Engine torque. (c) Total particle number concentration during tests using BP-15. (d) Total particle number concentration during tests using Certification Fuel.

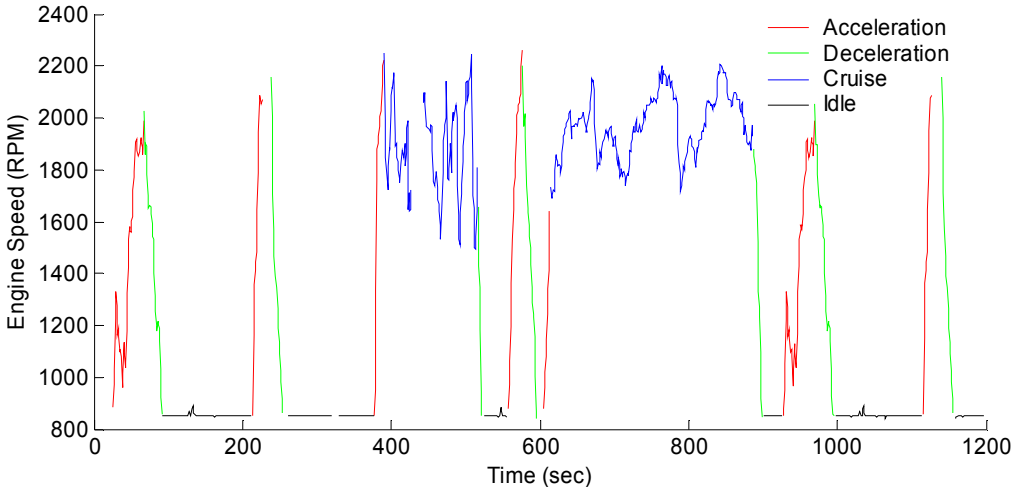

Figure 2: Different engine operation modes during the FTP transient test cycle.

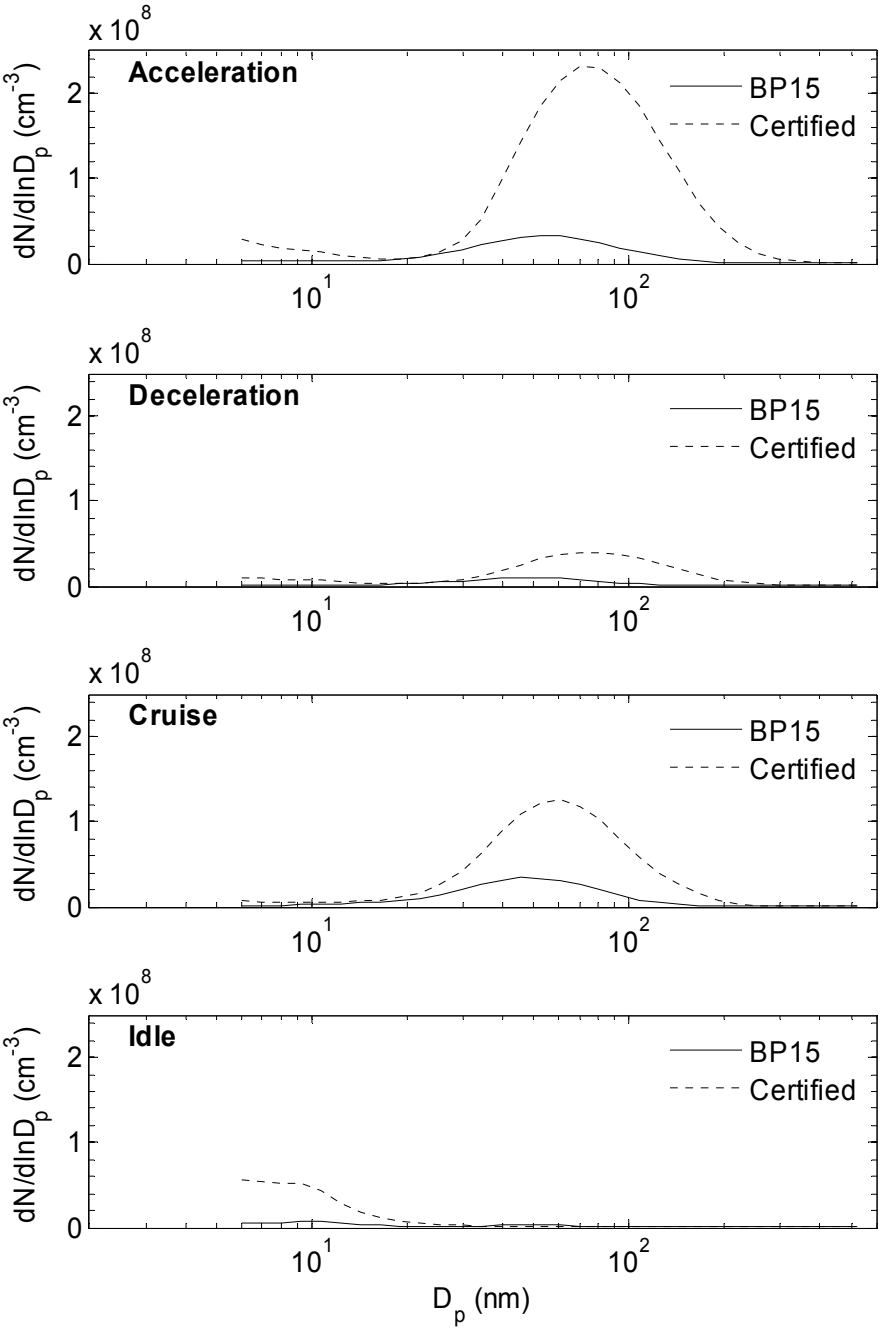

Figure 3: Particle number size distributions averaged over individual operation modes for tests using BP-15 and Certification Fuel.

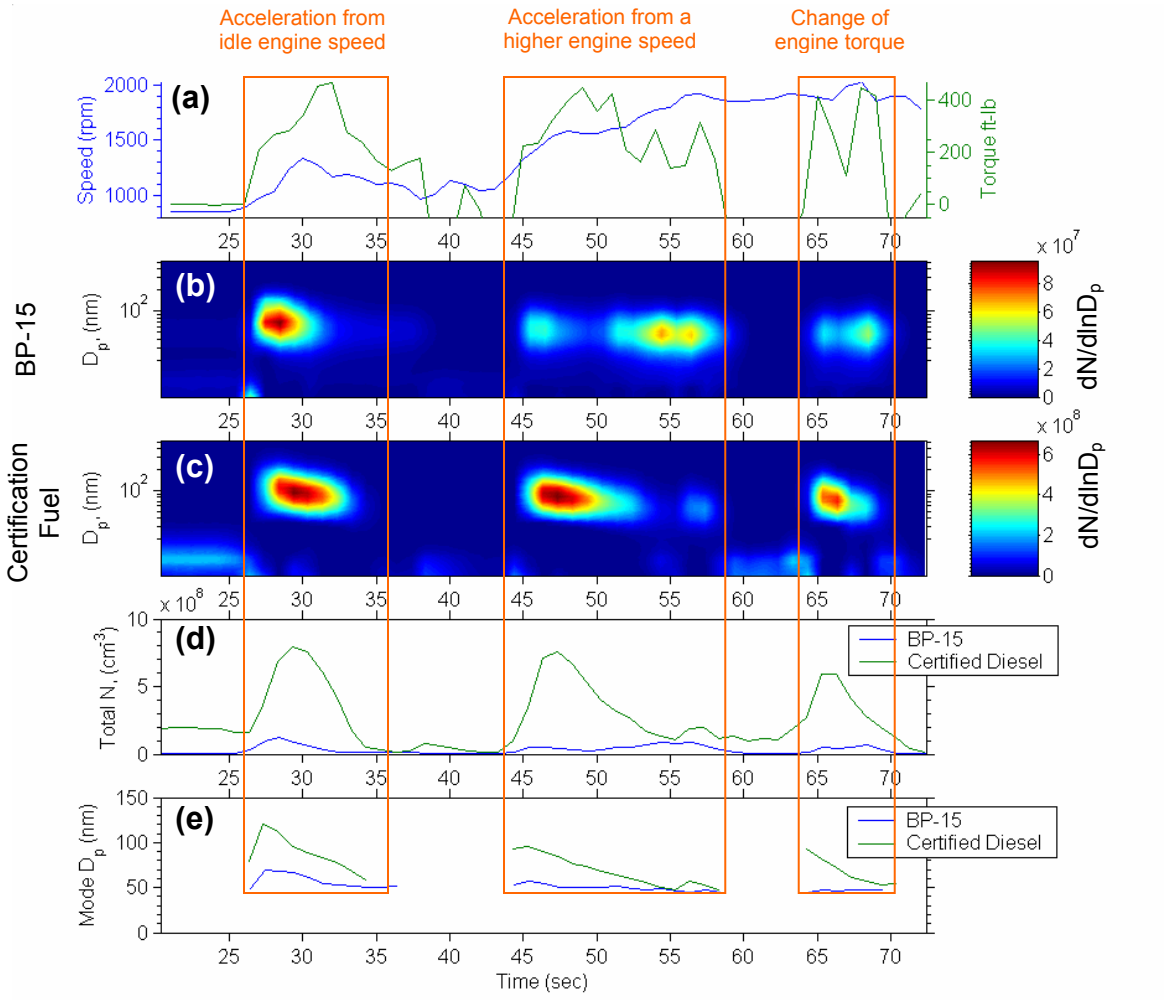

Figure 4. Time series of engine parameters and particle emission measurements during a typical acceleration period. (a) Engine speed and torque. (b) Particle number size distribution during a test with BP-15. (c) Particle size distribution during a test with Certification Fuel. (d) Total particle number concentrations during tests using BP-15 and Certification Fuel; (d) Aitken mode diameters of particle size distributions.

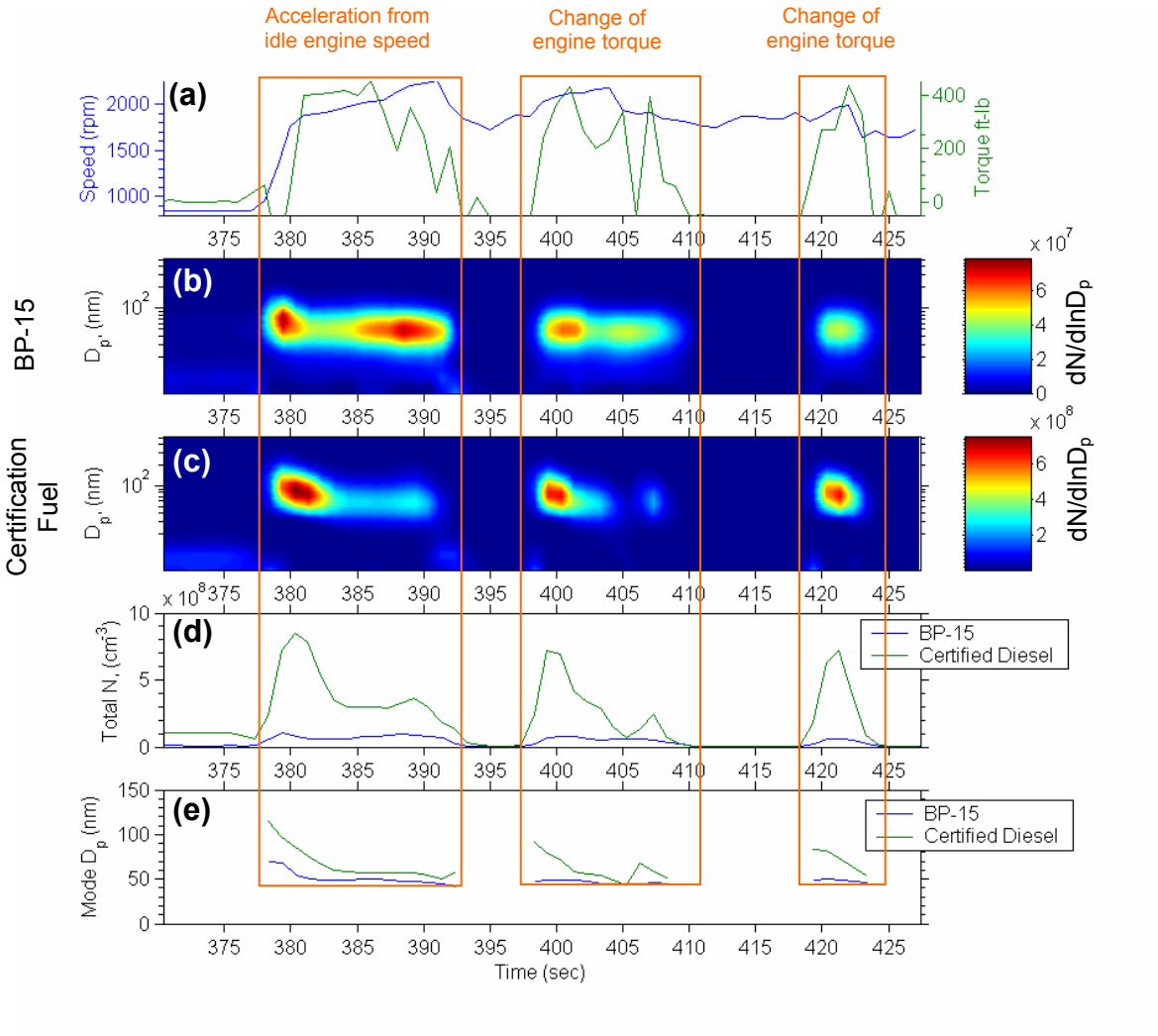

Figure 5. Time series of engine parameters and particle emission data during a typical "cruise" period following acceleration from idling. (a) Engine speed and torque. (b) Particle number size distribution during a test with BP-15. (c) Particle number size distribution during a test with Certification Fuel. (d) Total particle number concentrations during tests using BP-15 and Certification Fuel; (d) Aitken mode diameters of particle size distributions.

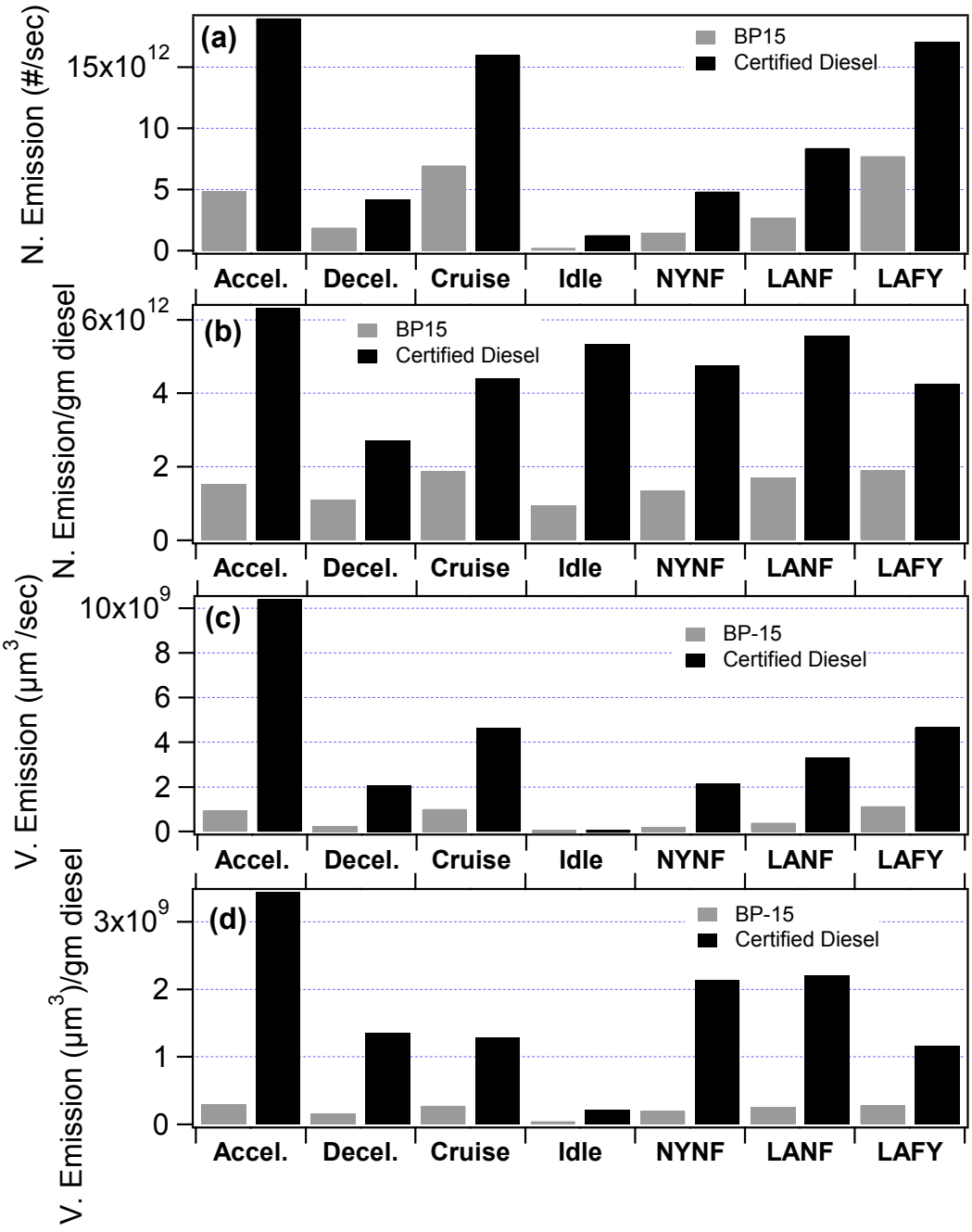

Figure 6: Emission rates averaged over each operation mode and phase of the FTP transient test cycle. (a) Number emission rate (#/sec). (b) Volume emission rate (μm^3/sec). (c) Number emission per unit diesel fuel consumed (#/g); (d) Volume emission per unit fuel consumed (μm^3/g)

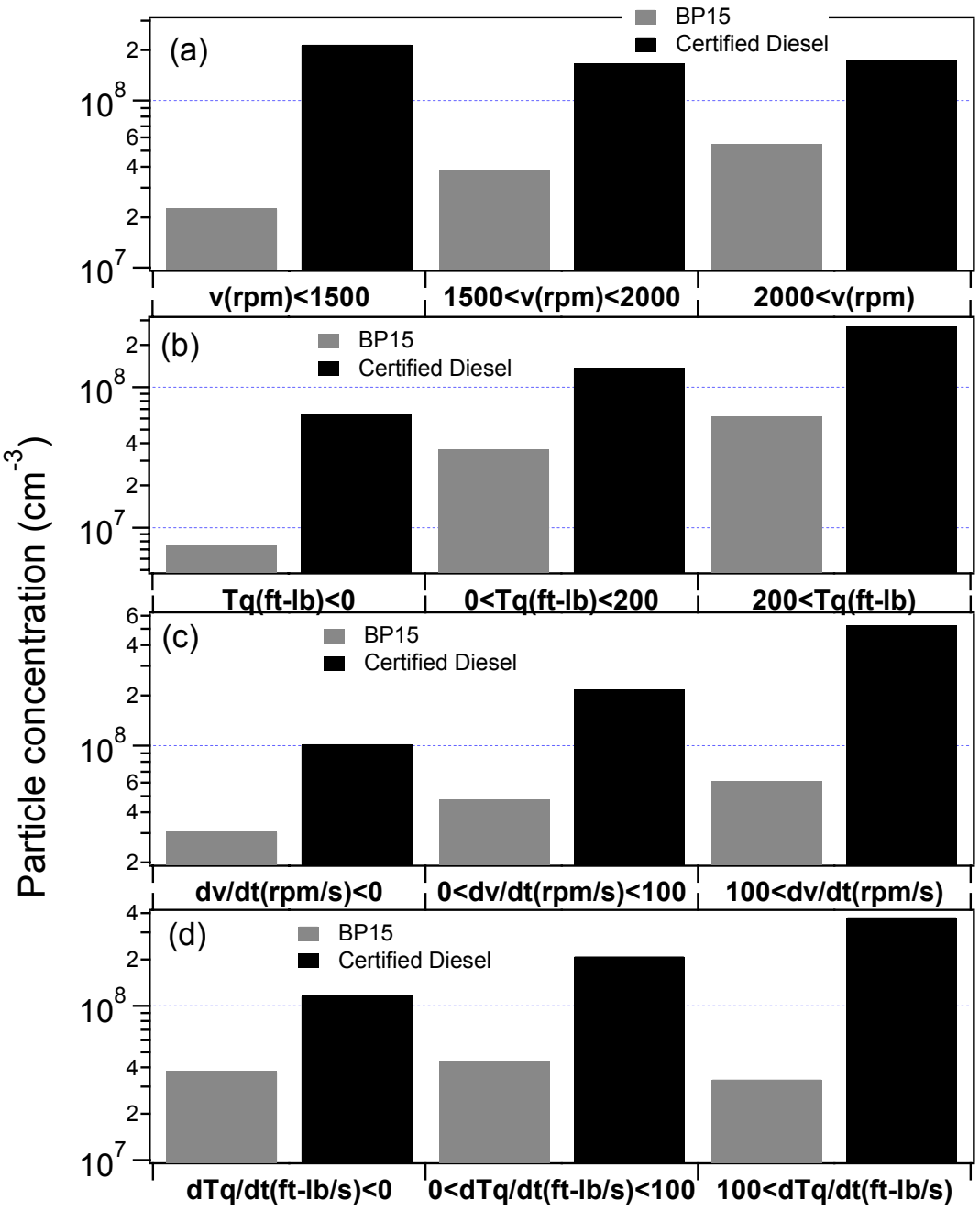

Figure 7: Particle number concentrations averaged over different ranges of (a) engine speed, (b) engine torque, (c) acceleration *dv/dt*, and (d) change rate of engine torque *dTq/dt*.

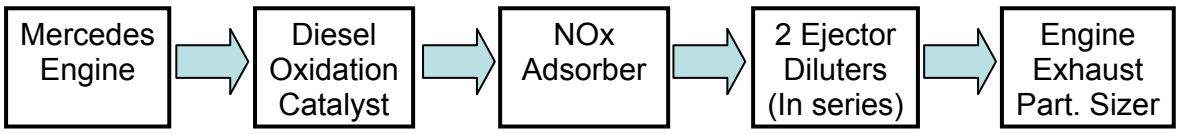

Figure 8. Schematic of the experiment setup for particle sampling during active regenerations of a NOx adsorber.

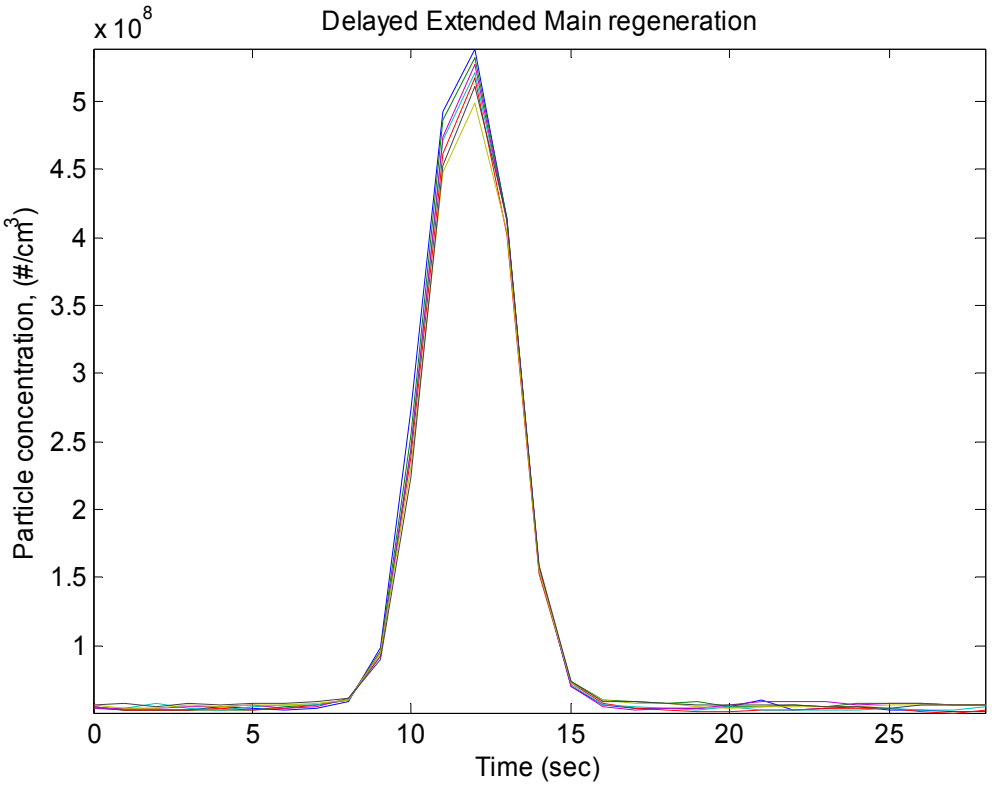

Figure 9. Test to test variability of the transient particle number concentration during Delayed Extended Main regeneration. Particle number concentrations were integrated over the size range of particle size distributions measured by the EEPS.

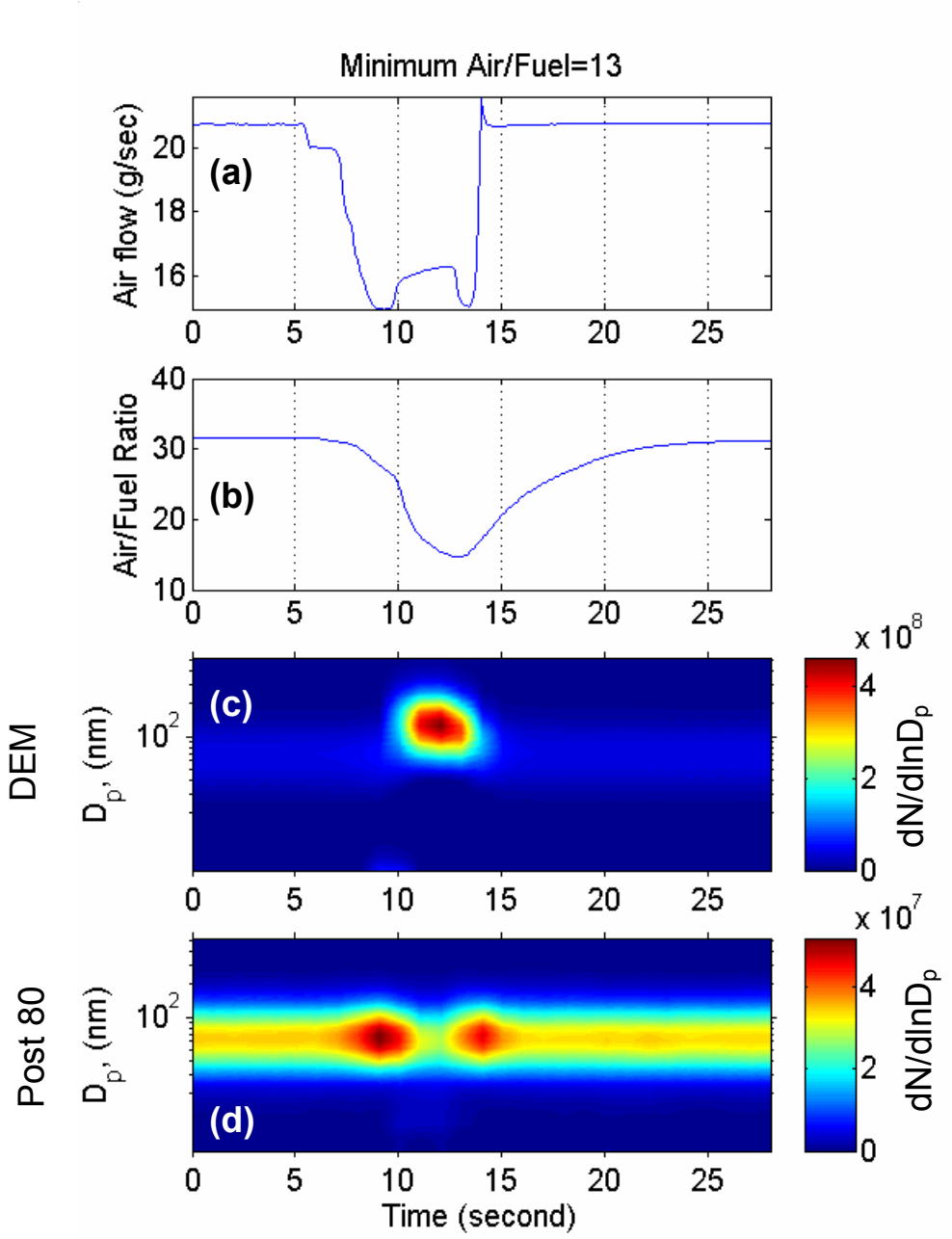

Figure 10. Time series of engine control parameters and particle size distributions during NOx adsorber active regenerations. (a) Engine air flow rate. (b) Air to fuel flow ratio. (c) Particle number size distribution during a DEM regeneration. (d) Particle number size distribution during a Post80 regeneration. The minimum air to fuel flow ratio was 13 during the regenerations.

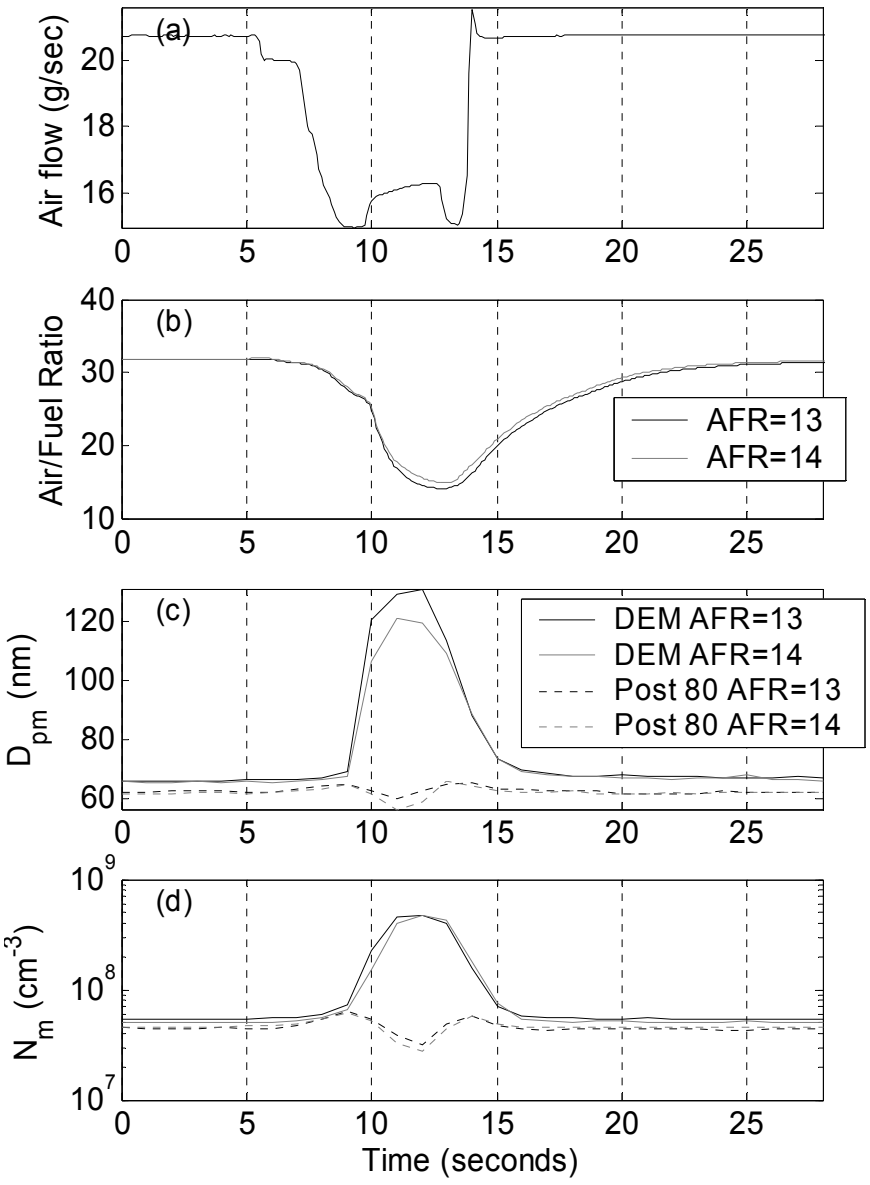

Figure 11. Time series of (a) engine air flow rate, (b) air to fuel flow ratio, (c) fitted mode diameters, and (d) fitted mode concentrations of particle size distributions measured during active regeneration experiments.